Experimental Study on the Performance of a Turbopump Inducer

Soon-Sam Hong, Jin-Sun Kim, Chang-Ho Choi, Jinhan Kim
Korea Aerospace Research Institute
45 Eoeun-Dong, Youseong-Gu, Daejeon 305-333, Korea
sshong@kari.re.kr

Keywords: Turbopump, Inducer, Performance, Cavitation

Abstract

Characteristics of steady and unsteady cavitation in a turbopump inducer were investigated in this paper. To see the effect of tip clearance on the inducer performance, three cases of tip clearance were tested. The helical inducer, which has two blades with inlet tip blade angle of 7.8 degree and tip solidity of 2.7, was tested in the water. In the non-cavitating condition, the inducer head decreased with increase in the tip clearance. Rotating cavitation and cavitation surge were observed through unsteady pressure measurements at the inducer inlet. The cell number and propagation speed of the rotating cavitation were determined through cross-correlation analysis. During the rotating cavitation one cell rotated at the same rotational speed as that of the inducer rotation and the cavitation surge did not rotate. The critical cavitation number increased with increase in the tip clearance at the same flow rate, but the change of critical cavitation number was small at the nominal flow rate.

Introduction

Turbopump is used to supply the combustion chamber with the fuel and oxidizer in the liquid rocket engine. The objective of an inducer is to pressurize the flow sufficiently to enable the main centrifugal impeller to operate without the dangerous cavitation. Many studies[1-6] have been made on the inducer cavitation and depend mostly on the experiments due to the difficulties in the analysis and prediction. Recently some papers[1-4] were published on the unsteady cavitation phenomena such as rotating cavitation, cavitation surge, etc.

Steady state performance of an inducer was measured in the various solidities[5] and various blade angles[6] from the viewpoint of design parameters. Unsteady cavitation such as rotating cavitation and cavitation surge, which were observed in a turbopump inducer, were investigated in this paper. The effect of the radial tip clearance is also presented.

Experimental Apparatus

An outline of the test loop is shown in Fig. 1. The impeller was driven by a variable speed motor. The flow rate was controlled by a regulating valve. The pressure of the water tank was adjusted by using a vacuum pump and the compressed air. A booster pump was operated when the inducer head was not high enough to circulate water the test rig. The booster pump has no effect on the inducer performance.

The geometry and operating condition of the test inducer are shown in Table 1. The inducer, which is shown in Fig. 2, has the inlet tip diameter of 106 mm and two blades. Three cases of the tip clearance, which is defined as the radial gap between the inducer tip and the casing, were tested by using three casings with different inner diameter for the same test inducer. Clearance ratio c/H is defined as the ratio of the clearance c to the inlet blade height H, where H is the inducer radius minus the shaft radius. The baseline clearance was 1.0 mm, which corresponds to the clearance ratio c/H = 0.026. The inlet flow coefficient ϕ is defined as the ratio of mean axial velocity at inducer inlet to the tip speed at inducer inlet.

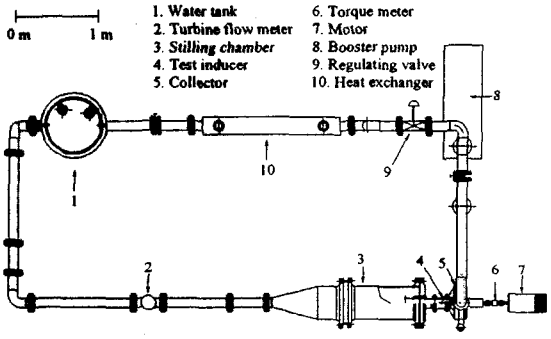

Fig. 1 Plane view of test loop

Table 1 Inducer geometry and operating condition

Radial clearance, c [mm]	1.0	2.0	3.0
Inlet blade height, H [mm]	38		
Clearance ratio, c/H	0.026	0.053	0.079
Inlet tip diameter [mm]	106		
Outlet tip diameter [mm]	78		
Inlet tip blade angle [°]	7.8		
Outlet tip blade angle [°]	13.2		
Blade number	2		
Tip solidity	2.7		
Axial length of blade on the hub [mm]	88		
Rotational speed [rpm]	6,000		
Nominal flow rate Q_n at 6000 rpm [L/s]	20.5		
Inlet flow coefficient at nominal flow rate	0.073	0.070	0.067

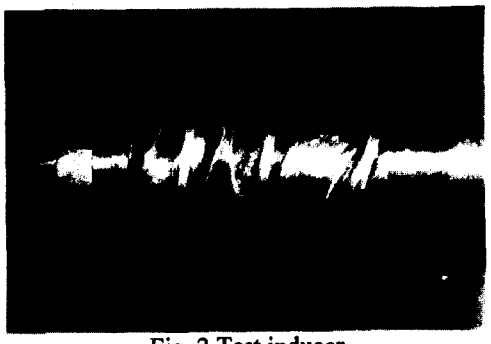

Fig. 2 Test inducer

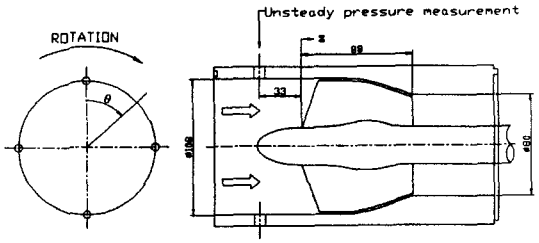

Fig. 3 Inducer test section and unsteady pressure measurement location

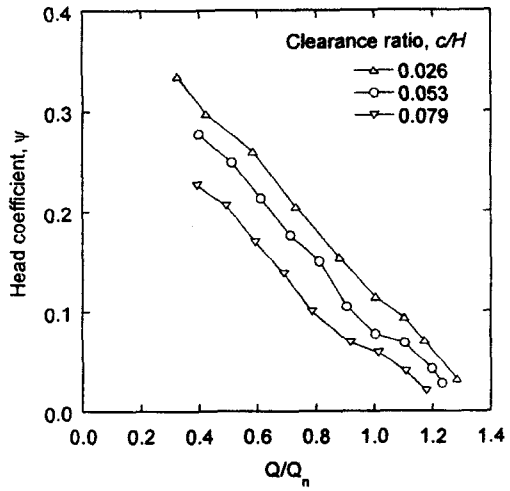

Fig. 4 Head characteristics of inducer

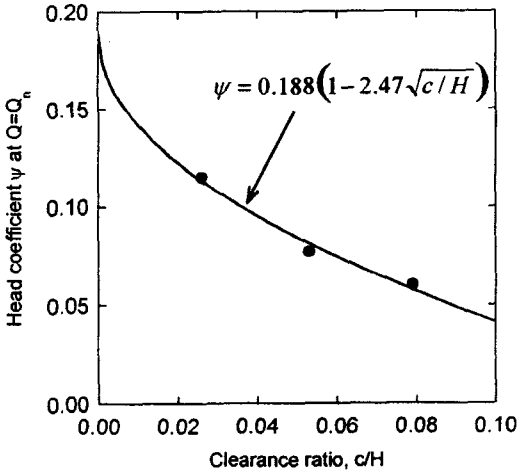

Fig. 5 Head versus tip clearance at nominal flow rate

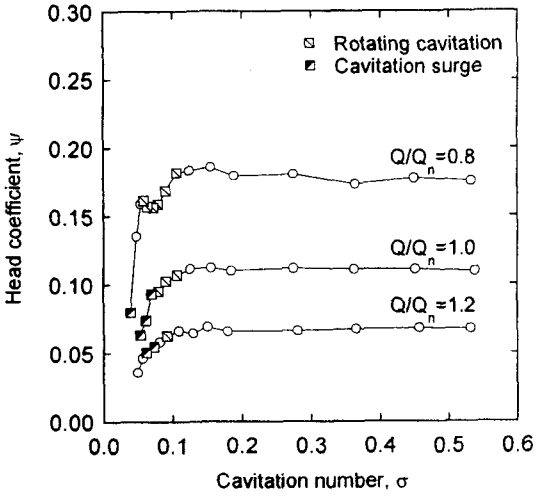

(a) c/H=0.026

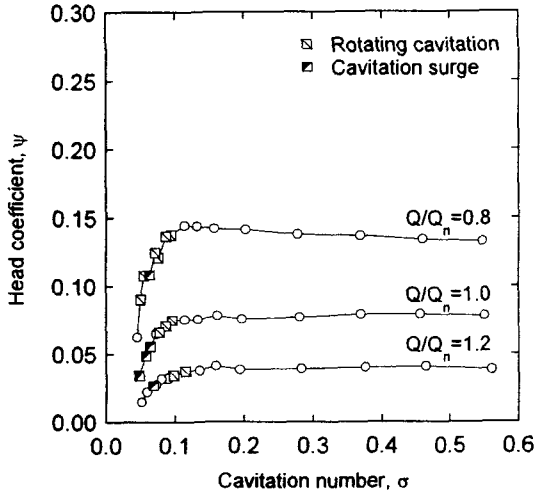

(b) c/H=0.053

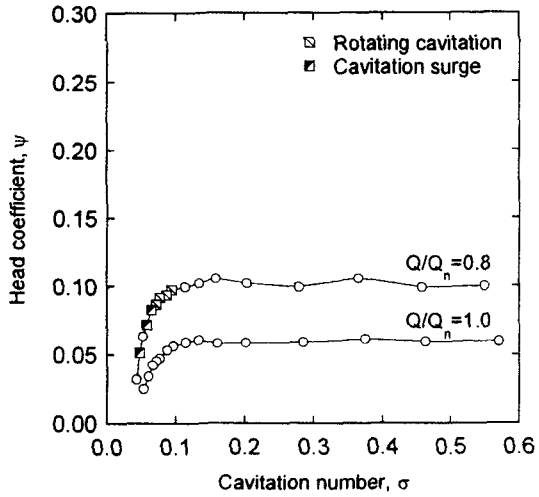

(c) c/H=0.079

Fig. 6 Cavitation performance curve of inducer

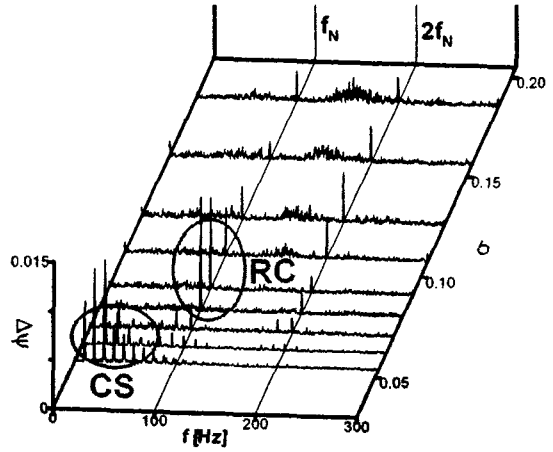

Fig. 7 Spectral analysis of inlet pressure fluctuation for c/H=0.026 at $Q=Q_n$: *RC* is rotating cavitation and *CS* is cavitation surge

The rotational speed of the inducer was fixed at 6,000 rpm for the present study. The mean flow rate was measured by a turbine-type flow meter. The inducer head was evaluated from the pressure difference between the inlet stilling chamber and collector outlet. Four fast-response pressure transducers (Kulite ETM-375 model) were installed 33 mm upstream of the inducer, at four circumferential locations at 90-degree intervals as shown in Fig. 3.

Results and Discussions

Head coefficient ψ versus flow rate ratio Q/Q_n of the inducer is shown in Fig. 4. Q_n is the nominal flow rate of the inducer and head coefficient ψ is,

$$\psi = H/(U_{1t}^2/2g) \tag{1}$$

where U_{1t} is tip speed at inducer inlet, and H is total head of inducer. Head coefficient decreased linearly with flow coefficient. At nominal flow rate the head coefficient decreased with tip clearance. A study indicates that the loss in performance may be estimated from the following empirical relationship[7]:

$$\psi = \psi_0\left(1 - k\sqrt{c/H}\right) \tag{2}$$

ψ_0=0.188 and k =2.47 were obtained from the curve fitting of the test result, as shown in Fig. 5.

Cavitation characteristics of the inducer were presented in Fig. 6 for three cases of tip clearance. The cavitation number σ is defined as $NPSH/(U_{1t}^2/2g)$. Data for c/H=0.079 at Q/Q_n =1.2 was not available due to the system loss of the test loop. In Fig. 6 points for unsteady cavitation such as rotating cavitation and cavitation surge are marked. To investigate these unsteady cavitation phenomena, spectral analysis of the inlet pressure fluctuation at c/H=0.026 and $Q=Q_n$ are done and presented in Fig. 7. The ordinate $\Delta\psi$ is the inlet pressure fluctuation normalized by $0.5\rho U_{1t}^2$.

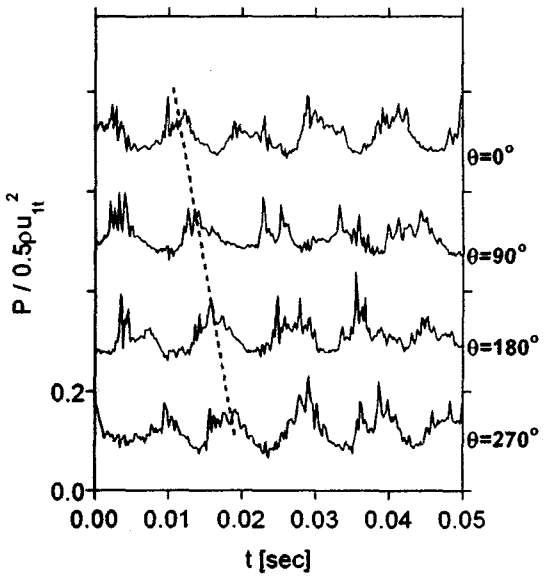

(a) Pressure signal at four circumferential locations

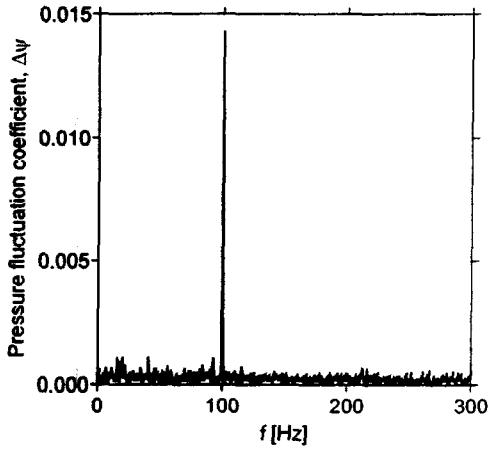

(b) Spectrum of inlet pressure fluctuation at θ=0°

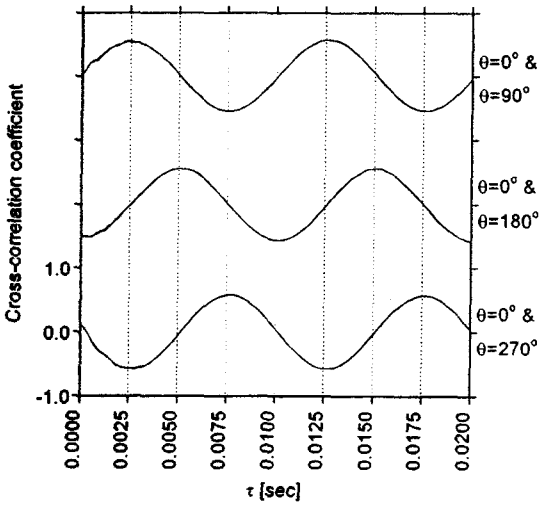

(c) Cross-correlation coefficients

Fig. 8 Inlet pressure at rotating cavitation for c/H=0.026 at σ=0.08, $Q=Q_n$

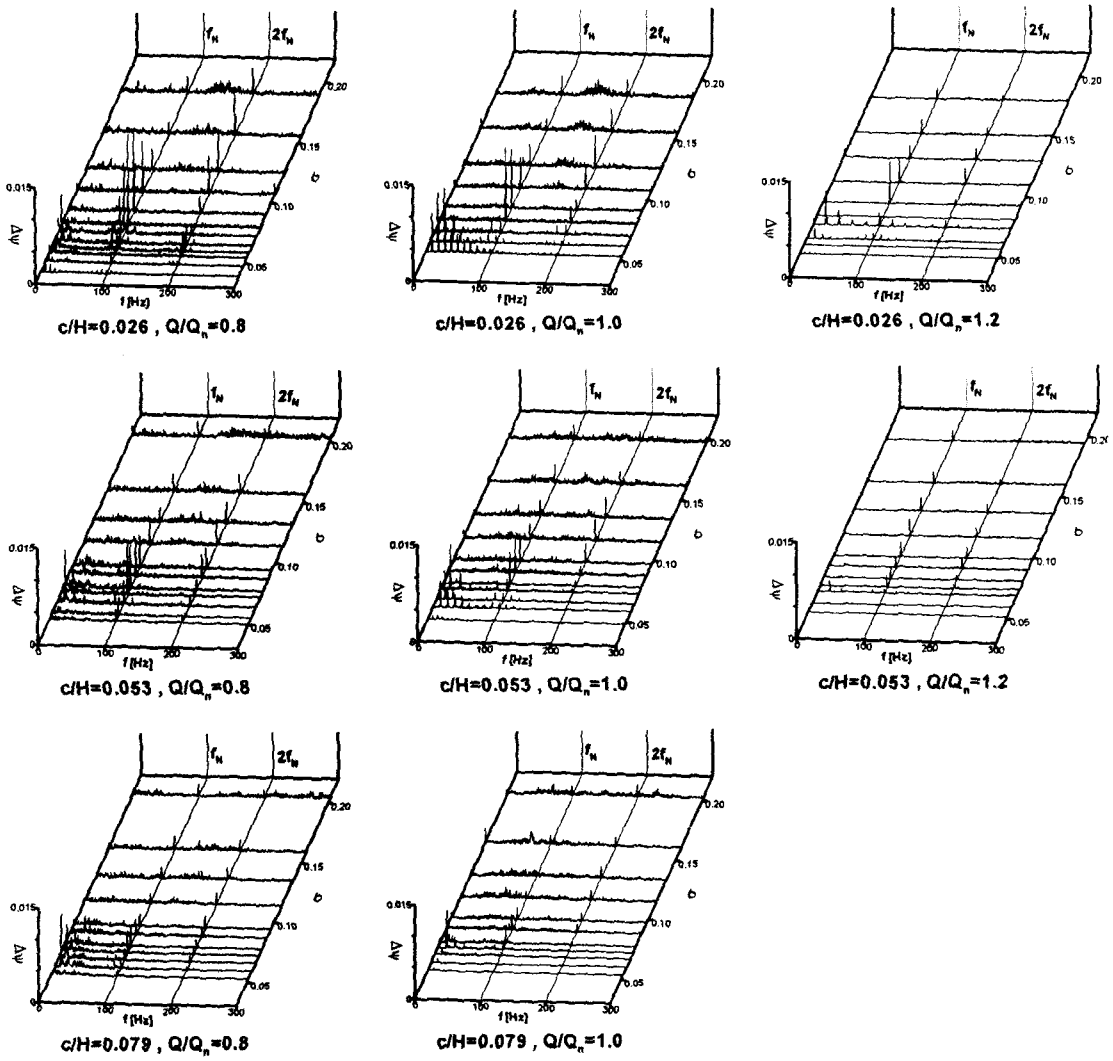

Fig. 9 Spectral analysis of inlet pressure fluctuations at three cases of tip clearance

In Fig. 7, f_N is the rotational frequency (=100 Hz) of the inducer, and the data are displayed at the region of cavitation number σ<0.2 of Fig. 6(a). While the cavitation number σ being decreased, rotating cavitation was observed at σ=0.107. The cell number and frequency of the rotating cavitation will be identified later on. With further decrease in σ cavitation surge, where the pipeline system including the test inducer oscillated at frequency range of 10-15 Hz, was observed at $\sigma \leq 0.07$.

Cross-correlation coefficients of unsteady pressure signals, which were obtained from four unsteady pressure transducers installed at the inducer inlet, were analyzed to see if the cavitation rotated or not. An example of the analysis is shown in Fig. 8, which corresponds to c/H=0.026 at σ=0.08 and Q=Q_n. Time signals of four unsteady pressure are shown in Fig. 8(a), where the ordinate is the normalized absolute pressure measured at the inducer inlet. A time lag is observed at the adjacent two signals, which means that the pressure pattern rotates circumferentially. Fourier transform of the pressure signal at θ=0 deg is shown in Fig. 8(b), where 100 Hz is the dominant frequency. Cross-correlation coefficients of pressure signals at θ=90 deg, 180 deg, 270 deg, compared to the signal at θ=0 deg, are shown in Fig. 8(c).

Cell number and propagation speed of the rotating cavitation were determined from the following formula[8],

$$m = \frac{2\pi}{\Delta\theta} \cdot \frac{\tau_1}{\tau_2} \tag{3}$$

$$f_s = \frac{1}{m\tau_2} \tag{4}$$

where m is number of cells, $\Delta\theta$ is the angle difference between two sensors, τ_1 is time lag between two signals, τ_2 is period of periodic signal at two sensors,

Table 2 Cell number and propagation speed ratio

		Cell number, m			Rotational speed ratio, f/mf_N		
c/H		0.026	0.053	0.079	0.026	0.053	0.079
Rotating cavitation		1	1	1	1.0	1.0	1.0
Cavitation surge	Q/Q_n= 0.8	0	0	0	7Hz	13Hz	8-12Hz
	Q/Q_n= 1.0				10-15Hz	7-15Hz	13Hz
	Q/Q_n= 1.2				12-20Hz	18Hz	

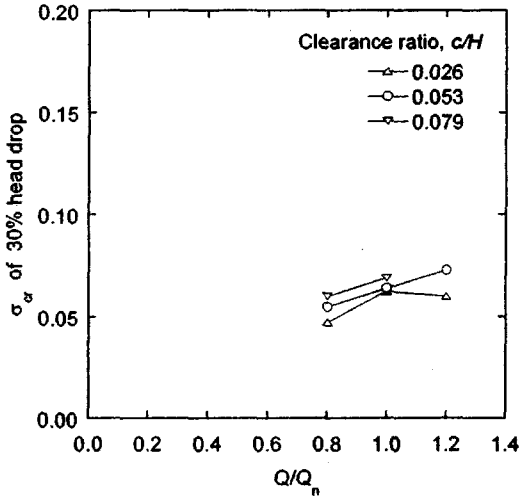

Fig. 10 Critical cavitation number versus flow rate

and f_s is angular propagation speed of the cells. This method revealed that one cell rotated at 100 Hz, which is the same frequency as the inducer rotational frequency, or 6,000 rpm (=100 Hz), in case of pressure signals at Fig. 8(c). Cavitation surges in Fig. 6 were found not to rotate from the cross-correlation analysis.

Fourier transforms of the signals at each flow rate for three cases of tip clearance are shown in Fig. 9. In case of *c/H*=0.026, the pressure fluctuation amplitude of rotating cavitation increased and that of cavitation surge decreased when Q/Q_n decreased from 1.0 to 0.8. Pressure fluctuation amplitude was on the whole lower than that at Q/Q_n =0.8, 1.0. The pattern of pressure fluctuation amplitude at *c/H*=0.053 was similar to that at *c/H*=0.026. At *c/H*=0.079, however, pressure fluctuation amplitude decreased noticeably. It was found that for three cases of tip clearance one cell of rotating cavitation rotated at 100 Hz, which was the same frequency as the inducer rotation, and that cavitation surge did not rotate. Characteristics of the unsteady cavitation are summarized at Table 2.

In Fig. 10 is presented the critical cavitation number, which is derived from the cavitation performance curves of Fig. 6. The critical cavitation number σ_{cr} is defined as the cavitation number where the head drops by 30 % of the head at non-cavitating condition. The critical cavitation number on the whole increased with increase in the flow rate. At the same flow rate the critical cavitation number increased with increase in the tip clearance, but the tip clearance had very small effect on the cavitation number at the nominal flow rate.

Conclusion

Three cases of tip clearance were tested in a turbopump inducer. At non-cavitating condition, the inducer head linearly decreased with flow rate and the head decreased with increase in the tip clearance. At cavitating condition, rotating cavitation and cavitation surge were observed in all cases of tip clearance. During the rotating cavitation, one cell rotated at the same rotational speed as that of the inducer rotation. The cavitation surge did not rotate and its oscillating frequency was 7~20 Hz. At the same flow rate the critical cavitation number increased with increase in the tip clearance, but the change of critical cavitation number was small at the nominal flow rate.

References

1) Lee, S., Jung K., Kim, J., Kang, S.: Cavitation Mode Analysis of Pump Inducer, *KSME International Journal*, **16**, 2002, pp. 1497-1510.
2) Tsujimoto Y., Yoshida. Y., Maekawa, Y., Watanabe, S., Hashimoto, T.: Observations of Oscillating Cavitation of an Inducer, ASME *Journal of Fluids Engineering*, 1997, **119**, pp. 775-781.
3) Furukawa, A., Ishizaka, K., Watanabe, S.: Experimental Study of Cavitation Induced Oscillation in Two Bladed Inducers, 4th International Conference on Launcher Technology, Space Launcher Liquid Propulsion, Liege, Belgium, 2002.
4) Yoshida, Y., Tsujimoto, Y., Kataoka, D., Horiguchi, H., Wahl, F.: Effect of Alternate Leading Edge Cutback on Unsteady Cavitation in 4-Bladed Inducers, ASME *Journal of Fluids Engineering*, **123**, 2001, pp. 762-770.
5) Hong, S., Koo, H., Choi, C., Cha, B., Yang, S.: Effect of Geometry on the Performance of Turbopump Inducer (in Korean), Proceedings of the KSME Fall Conference, 2002, pp. 1997~2002.
6) Kim, J., Hong, S., Choi, C., Kim, J., Cho, K.: Effect of Blade Angle on the Performance of Turbopump Inducer (in Korean), Proceedings of the KSAS Fall Conference, 2003, pp. 1059~1062.
7) Anon.: *Liquid Rocket Engine Turbopump Inducers*, Space Vehicle Design Criteria Monograph, 1971, NASA SP-8052.
8) Frigne, P., Van Den Braembussche, R.: Distinction between Different Types of Impeller and Diffuser Rotating Stall in a Centrifugal Compressor with Vaneless Diffuser, ASME *Journal of Engineering for Gas Turbines and Power*, **106**, 1984, pp. 468-474.